



Cite this: *New J. Chem.*, 2021, 45, 6220

Synthesis and structure of thienyl Fischer carbene complexes of Pt^{II} for application in alkyne hydrosilylation†

Zandria Lamprecht,^a Frederick P. Malan,^a Simon Lotz^a and Daniela I. Bezuidenhout^{*,b}

Transmetalation of group 6 thienylene Fischer carbene complexes to Pt^{II} precursors yielded new examples of neutral platinum(II) bisethoxycarbene complexes with either 2-thienyl (T) or 5-thieno[2,3-*b*]thienylene (TT) carbene substituents. The use of analogous aminocarbene group 6 precursors proceeded to give isomeric platinum(II) product mixtures where the resultant bisaminocarbene ligands displayed different orientations due to restricted rotation around the Pt–aminocarbene bond caused by the sterically demanding TT substituents. The well-defined Pt^{II} ethoxycarbene complexes were screened as catalyst precursors in the benchmark hydrosilylation reaction employing phenylacetylene and triethylsilane substrates. Marked selectivity for the β -*E* isomer (*E*-triethyl(styryl)silane) was observed, and the (pre)catalysts proved recyclable, active in solvent-free reactions, and displaying a high alkyne functional group tolerance.

Received 15th February 2021,
Accepted 15th March 2021

DOI: 10.1039/d1nj00791b

rsc.li/njc

Introduction

Acyclic heteroatom-stabilized carbene complexes of platinum(II) have been known since 1915,^{1–3} and yet the number of isolated examples are limited. In general, there are four methods available to prepare Pt^{II} Fischer carbene complexes (FCCs). Firstly, ligand modification of Pt^{II} isocyanide precursors with alcohols or primary amines produces the corresponding acyclic aminoxy- or diamino-carbene Pt^{II} complexes, respectively (Fig. 1a).⁴ Cationic alkoxy-carbene complexes can be prepared by reacting the Pt^{II} precursors with alkynes (Fig. 1b), to yield the π -bonded intermediates that lead to carbene formation after alkyne modification,⁵ while neutral bisalkoxycarbene complexes are obtained from the reaction of SiMe₃-substituted alkynes and H₂PtCl₆·6H₂O (Fig. 1c).⁶ The first transmetalation reactions from group 6 transition metal FCCs to produce mononuclear Pt-biscarbene complexes employed [PtCl₂(MeCN)₂] or PtCl₂ precursors (Fig. 1d) and the products were stabilized by amine-chelate formation.⁷

We have recently prepared Pt^{II} multicarbene complexes (Fig. 1e) by carbene transfer reactions of the ethoxy- and aminocarbene

ligands of W(0) FCCs to a Pt^{II} centre.⁸ The major products obtained from the reactions with group 6 carbene precursors are neutral bisethoxycarbene complexes of Pt^{II} and cationic mononuclear trisaminocarbene complexes (Fig. 1e). In this study, Pt^{II} Fischer carbene complexes with (annulated) thiophene substituents, are synthesized for the first time employing the methodology of carbene transfer, and their use as catalysts for the alkyne hydrosilylation reaction is investigated. Hydrosilylation of terminal alkynes is one of the leading methods to produce organosilanes, and is catalysed by many transition metals including platinum.^{9–18} Although Pt^{II} complexes containing N-heterocyclic carbene (NHC)

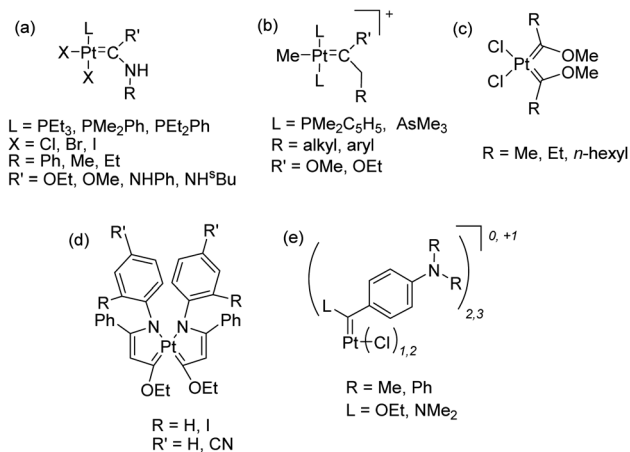


Fig. 1 Heteroatom-stabilized FCCs of platinum(II).

^a Department of Chemistry, University of Pretoria, Private Bag X20, Hatfield 0028, Pretoria, South Africa

^b Laboratory of Inorganic Chemistry, Environmental and Chemical Engineering, University of Oulu, P. O. Box 3000, 90014 Oulu, Finland.

E-mail: daniela.bezuidenhout@oulu.fi

† Electronic supplementary information (ESI) available: Synthesis details, NMR, crystal data collection, structure refinement, crystal packing details and hydrosilylation catalysis details. CCDC 2061163–2061168. For ESI and crystallographic data in CIF or other electronic format see DOI: 10.1039/d1nj00791b



ligands are commonly employed as catalysts for this reaction,^{9,12,18} no Fischer carbene catalysts have been reported.

Results and discussion

Synthesis of platinum(II) FCCs

Pt^{II} multicarbene complexes were synthesized by transmetalation reactions of the chromium or tungsten carbonyl FCC precursors **P1–P4**, containing either a 2-thienyl (T) or a 5-thieno[2,3-*b*]thienylene (TT) substituent (see Experimental section and ESI† for the preparation of **P1–P4**), *via* a modified procedure of that reported by Sierra and co-workers (Scheme 1).⁷ Transmetalation occurred by stirring a group 6 FCC with a platinum precursor for 24–30 h in refluxing dichloromethane (DCM). The syntheses of Pt^{II} FCCs are facile, but purification of the compounds proved challenging. The complexes are light sensitive, insoluble in most solvents (*e.g.* dichloromethane, chloroform, acetonitrile) and chromatographic purification processes are compromised. Four Pt^{II} biscarbene complexes were successfully isolated, namely *cis*-[PtCl₂{C(OEt)-2-C₄H₃S₂}₂] (**1**), *cis*-[PtCl₂{C(OEt)-5-C₆H₃S₂}₂] (**2**), *cis*-[PtCl₂{C(NH₂)-5-C₆H₃S₂}₂] (**3a/b**) and *cis*-[PtCl₂{C(NMe₂)-5-C₆H₃S₂}₂] (**4a/b**) (Fig. 2). The transmetalation reactions do not run to completion, even with prolonged reaction times, and starting material is recovered from all reactions.

The *cis*-biscarbene complexes of **3** and **4** have three isomeric possibilities where the TT spacers and amino fragments have various orientations to yield different geometric stereoisomers (Fig. 2) due to restricted rotation enforced by the sterically demanding thieno[2,3-*b*]thienylene carbene substituent and the amino group with increased C_{carbene}–N bond order. Evidence for the formation of two out of the possible three isomers is observed for **3** and **4**. In addition, the formation of a cationic Pt triscarbene complex ([PtCl{C(NMe₂)-5-C₆H₃S₂}₃]Cl, **4d**) is observed for the reactions done with group 6 transition metal dimethylaminocarbene complexes. The orientation of the carbene substituents in **4d** is unknown.

Compounds **3** were synthesized using **P3_W** (see ESI,† Fig. S1) and Pt(COD)Cl₂ in DCM. The *cis* isomer **3** was obtained with evidence for the isolation of two-out-of-three possible geometric

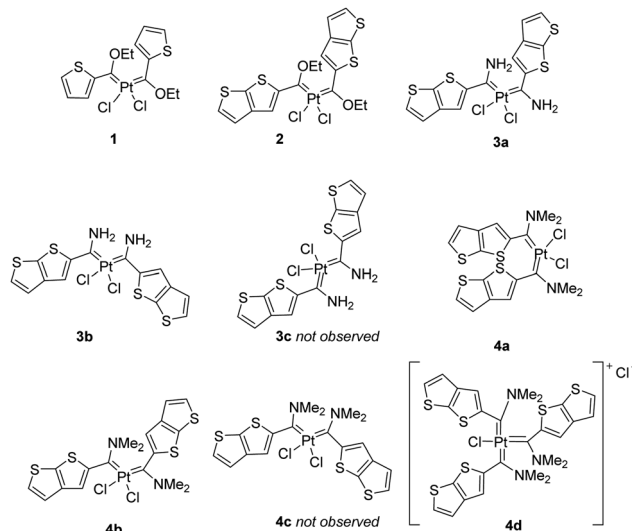


Fig. 2 Pt^{II} Fischer carbene complexes **1–4**.

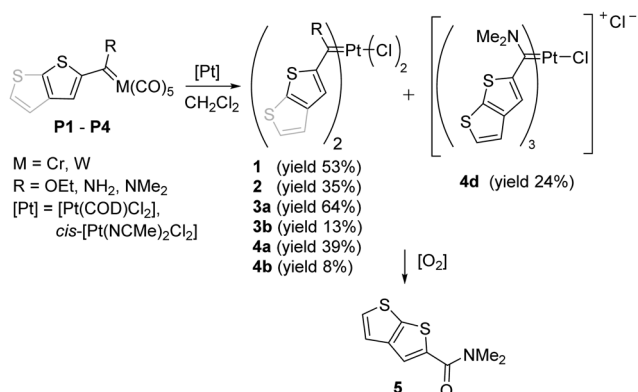
stereoisomers that are inseparable. The two isomers are **3a** (yield 64%) and **3b** (yield 13%), obtained in the ratio 5 : 1 as determined by integrating the ¹H NMR spectrum resonances (ESI,† Fig. S9).

Compounds **4** were isolated from transmetalation reactions using **P4_{Cr/W}** along with Pt(COD)Cl₂ or *cis*-[PtCl₂(NMe₂)₂] in DCM. The preferred reaction conditions are employed by reacting **P4_{Cr}** with Pt(COD)Cl₂ in DCM, to produce **4** in 71% yield. Excess **P4_{Cr}** and Pt(COD)Cl₂ are removed by washing the reaction precipitate with minimal amounts of DCM, chloroform and ether. Two-out-of-three possible geometric stereoisomers of the *cis*-biscarbene complex of **4** are obtained.

The two isomers, **4a** (yield 39%) and **4b** (yield 8%), are accompanied by the triscarbene complex (**4d**, yield 24%) in the ratio 5 : 1 : 3 as determined by integrating ¹H NMR spectrum resonances (ESI,† Fig. S11). Compounds **4** only dissolve in DMSO and partly in chlorinated solvents (*e.g.* DCM and CDCl₃), hence the more insoluble **4d** could be purified by washing the precipitate with a variety of solvents. In an attempt to purify **4**, a short silica gel filter using acetone as eluent produced only the decomposition product (NMe₂)C(O)-5-C₆H₃S₂ (**5**, yield 24%).

The solubility of Pt^{II} FCCs decrease (**1** > **2**) with an increase in the number of thiophene units in the annulated spacer (**1** < **2**). A decrease in solubility is also seen when changing the heteroatom substituent from ethoxy- (**2**) to amino- (**3**, **4**).

The mechanism for obtaining a Pt^{II} mononuclear biscarbene complex from Pt(COD)Cl₂, requires the substitution of the η⁴-COD ligand, leaving two *cis* empty coordination sites on the metal. A stepwise mechanism is likely followed where the COD ligand remains partially coordinated (η²-COD), still bound to the metal through one of the two double bonds of cyclooctadiene, as the first carbene ligand coordinates.^{19,20} Coordination of the second carbene ligand, to the Pt^{II} metal, completely displaces the COD ligand. Further substitution would require that the *trans* effect of a carbene ligand is relatively stronger than that of a chloro ligand.⁸



Scheme 1 Fischer carbene ligand transfer to a platinum(II) metal centre.

Spectroscopic characterization

NMR spectra were recorded in CDCl_3 , CD_2Cl_2 and $(\text{CD}_3)_2\text{SO}$, depending on the solubility of the compounds. ^1H NMR data are summarized in Table 1. The aromatic proton adjacent to the carbene carbon is most affected by the coordination of the carbene fragment. In **1** this is seen in the resonance of H3 and even more so in H4 of **2** (ESI,† Fig. S6 and S7). Due to conjugation in the thiophene ring of **1**, H5 is also shifted significantly downfield. The methylene resonances of Pt^{II} ethoxycarbene complexes appear as broadened peaks instead of quartets. One such broad peak/unresolved quartet is observed in the ^1H NMR spectrum of **1** and two in the case of **2**, resonating *ca.* 0.6 ppm apart (Fig. S6 and S7, ESI†). Due to the bulky nature of thienylenes and the *cis*-orientation of the two carbene ligands in the square planar structure of the platinum complexes, the peak broadening is ascribed to restricted rotation of the OEt group around the carbene carbon, more pronounced in **2** (larger TT spacer) compared to **1** (T spacer). The broad signals of **2** are duplicated indicating different electronic environments for the ethoxy substituents. Recording the NMR spectrum of **2** in a different solvent, *e.g.* CD_2Cl_2 or at a lower temperature (2 °C) did not significantly improve the resolution of the spectra.

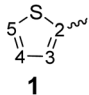
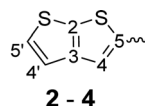
In the ^1H NMR spectrum of **3a**, a double duplication of the carbene ligand resonances is observed in a 1 : 1 ratio (ESI,† Fig. S9), for the compound **3b**. The two *cis*-biscarbene isomers are not separable. The difference between the two stereoisomers **3a** and **3b** can be visualized by restricting rotation around the $\text{Pt}-\text{C}_{\text{carb}}$ bond. In **3a** a structure is assigned whereby each amino substituent is on the same side as the sulphurs in the adjacent TT ring, of the two carbene ligands (Fig. 2). The 1 : 1 ratio of the aromatic proton resonances of **3b** indicates that the molecule constitutes of two different carbene ligands. In **3b** one ligand has the same conformation as the TT substituents in **3a**, but the other TT substituent is rotated around the $\text{C}_{\text{carb}}-\text{C}_{\text{TT}}$

bond to take up a position where the amino substituent is on the opposite side of the sulphurs in the TT ring. The greatest difference is observed for the NH and H4 proton resonances of **3a** and **3b**. Two significantly different NH resonances are observed, hence H-bonding interactions are suspected. Because three geometric stereoisomers are possible for **3** (Fig. 2), **3b** is expected to be one of the minor isomers. A third isomer **3c**, with both amino substituents on opposite sides of the sulphurs in the TT rings, was not observed.

In solution, the TT spacers may rotate and the major product (**3a**) is expected to be the energetically favoured compound where the amino groups are on the same side as the sulphurs of the TT-rings. This is also the favoured orientation for group 6 transition metal aminocarbene complexes.^{21,22} Compound **3b** is presumed to be the result of both intra- and intermolecular NH interactions and H-bonding interactions with polar solvents (DMSO- d_6 or THF), causing restricted rotation in the molecule. Single crystal X-ray diffraction confirms the molecular structure of this minor isomer **3b** (*vide infra*), and is obtained due to the preferential crystallisation of this compound. The possibility of a cationic triscarbene monochlorido Pt^{II} complex for **3**, similar to those reported earlier by us,⁸ is excluded due to the 1 : 1 integration of the carbene ligand's protons. Similarly, the *trans*-biscarbene isomer would be expected to yield only one set of duplicate signals and is therefore also ruled out as the possible product of **3b**.

^1H NMR spectra of mixtures of **4a**, **4b** and **4d** in CDCl_3 were recorded (ESI,† Fig. S11). DMSO was employed as a deuterated solvent for ^1H NMR spectroscopy of the least soluble, purified fraction **4d** (ESI,† Fig. S12). Poor resolution and peak broadening are observed for **4d**, ascribed to small differences in chemical shifts of protons as more than one of the same carbene ligand is present in the macromolecule, along with the impact of bulky carbene substituents restricting rotation in the molecule.

Table 1 ^1H NMR chemical shifts (δ) of the Pt FCCs

Complex							OEt ^d	NH ₂ /NMe ₂ ^e
	H3	H4	H5	H4'	H5'	H5'		
1 ^b	8.69	7.28	8.09				5.60, 1.59	
1 ^c	8.68	7.31	8.13				5.54, 1.59	
2 ^b		9.08		7.35	7.44		5.77, 5.18, 1.59	
2 ^c		9.03		7.39	7.49		5.73, 5.21, 1.58	
3a ^d		8.26		7.40	7.66			10.77, 10.61
3b ^d		8.56, 8.46		7.46, 7.43	7.73, 7.72			11.42, 11.18
4a ^b		8.06		7.35	7.45			4.22, 3.86
4a ^d		8.00		7.45	7.73			4.06, 3.77
4b ^b		7.61		7.29	7.38			3.30
4b ^d		7.80		7.41	7.70			4.15, 3.65
4d ^{df}		7.65, 7.37		7.26, 6.78	7.37, 6.87			4.10, 3.63, 3.38, 3.30

^a Proton chemical shifts for the ethoxy fragment are reported with the first value being the chemical shift of the methylene group, and the second the chemical shift of the methyl group. In the case of **2** there are two values for the methylene groups. ^b NMR data recorded in CDCl_3 . ^c NMR data recorded in CD_2Cl_2 . ^d NMR data recorded in $(\text{CD}_3)_2\text{SO}$. ^e Proton chemical shifts for the NH₂ fragments of **3a** and **3b**. In the case of **4** the chemical shifts represent the methyl groups of NMe₂. ^f Broadened resonances observed. The first values reported being the chemical shifts of the two carbene fragments opposite each other and the second the chemical shifts of the carbene fragment *trans* to a chloro ligand.



This is not uncommon especially for cationic triscarbene complexes of Pt^{II} with two carbene ligands *trans* to each other and one carbene ligand *trans* to Cl.⁸

Two of the three geometric isomers of the *cis*-biscarbene complex (**4a/b**, Fig. 2) are identified in the reaction mixture. The sharp, resolved signals of the biscarbene complexes are clearly distinguishable from the broadened signals of the triscarbene complex (Fig. S11, ESI†). The major *cis*-biscarbene isomer (**4a**) has the NMe₂ fragments rotated away from the sulphur atoms in the TT spacers and the minor isomer (**4b**) has the NMe₂ fragments rotated to the same side as the sulphur atoms in the TT spacers. A single crystal of **4a** could be isolated to confirm the molecular structure (*vide infra*). Hydrogen bonding interactions closer than 2.6 Å are absent in the solid state structure of **4a** and did not affect the rotations in the molecule. The third isomer **4c** with two different orientations of the NMe₂ fragments, would result in duplicated proton resonances in a 1 : 1 ratio (similar to **3b**), and is not observed. The individual proton resonances of **4a** are more downfield compared to **4b** (Fig. S11, ESI†). Two significantly different NMe₂ resonances are observed for **4a** in CDCl₃, *ca.* 0.3 ppm apart, that are more downfield compared to the single resonance of **4b** at 3.30 ppm (Table 1). In (CD₃)₂SO both NMe₂ fragments of **4a** and **4b** appear as two signals, respectively.

A cationic triscarbene complex structure for **4d** is further supported by the poorer solubility of the complex in deuterated solvents and the upfield shifts of the TT proton resonances when compared with the corresponding biscarbene complexes. In (CD₃)₂SO the 2 : 1 ratio of the two carbene ligands *trans* to each other and one carbene ligand *trans* to Cl are observed from proton integration 2 : 3 (2H + 1H) : 2 : 1 : 1 in the aromatic region (Fig. S12, ESI†), for the three thienothienylene carbene substituents. The resonances of the two *trans* carbene ligands are chemically equivalent and more downfield than the third carbene ligand (*trans* to Cl). The three NMe₂ fragments in **4d** resonate as four peaks (Table 1), with the two *trans* NMe₂ signals appearing as two broad signals (0.47 ppm apart) more downfield compared to the two broad signals of NMe₂ *trans* to Cl (0.08 ppm apart).

¹³C NMR data are summarized in Table 2. The carbene carbon chemical shifts of the Pt^{II} ethoxycarbene complexes (**1** and **2**) are at 235.2 and 233.2 ppm, respectively, comparable to the Pt^{II} ethoxy-FCC ([PtCl₂{C(OEt)-*p*-C₆H₄NMe₂}₂], 238.5 ppm in CD₂Cl₂).⁸ Compared to the carbene carbon signals of PtCl₂ bisalkoxycarbene complexes with aliphatic carbene substituents (Fig. 1c, *ca.* 278 ppm in CDCl₃)⁶ and mononuclear Pt-bisethoxycarbene complexes with cyclic amine substituents (Fig. 1d, *ca.* 198 ppm in CDCl₃),⁷ **1** and **2** are shifted significantly upfield and downfield, respectively. The carbene carbon chemical shift of **2** is *ca.* 36 ppm downfield from the corresponding signal in the analogue aminocarbene complex **3a** (196.5 ppm), measured in ((CD₃)₂SO); commensurate with the strong shielding effect of the amino-substituent of the carbene carbon atom, compared to an ethoxy substituent.⁸

Carbon chemical shifts are very similar in **1** and **2**, with the carbene carbon resonance slightly more downfield in **1**. The methyl

Table 2 ¹³C NMR chemical shifts (δ) of the Pt FCCs

Complex	C2	C3	C4	C5	C4'	C5'	C _{carb}	OEt ^b
1 ^a	150.5	145.4	130.4	142.5			235.2	80.5, 14.8, 14.8
2 ^a	^c	^c	140.2	153.6	122.1	131.9	233.2	80.1, 14.9
3a ^d	^c	^c	124.2	150.8	121.0	130.9	196.5	

^a NMR data recorded in CD₂Cl₂. ^b Carbon chemical shifts for the ethoxy fragment are reported with the first value being the chemical shift of the methylene group, and the second the chemical shift of the methyl group. ^c Assignments could not be made unambiguously. ^d NMR data recorded in (CD₃)₂SO.

resonance in **1** is duplicated. Broad signals are obtained for the carbene carbon and C4 resonance of **2** (ESI,† Fig. S8).

Compound **3b** was isolated as a mixture with **3a** as the major component and no ¹³C NMR data were obtained for this complex, or the insoluble **4d**. 2D NMR spectroscopy was employed to assign especially the aromatic resonances for the complex mixtures (ESI†).

Molecular structures

Crystallizations of the platinum(II) complexes **1**, **2**, **3b** and **4a**, precursor **P4_w** and the oxidized ester-product **5** were carried out from saturated DCM solutions of the compounds, layered with hexane. The structures of **P4_w** and **5** are reported in the ESI.† Due to the poor solubility of **3**, the compound was crystallized from a large amount of THF layered with hexane. Single crystal X-ray diffraction studies confirmed the molecular structures (Fig. 3). Selected bond lengths, angles and torsion angles are reported in Table 3, employing the atom numbering scheme as used in the NMR assignments. The single crystal X-ray diffraction data set for **2** is of too poor quality to publish, but the molecular structure is included in the ESI,† Fig. S19 to prove atom connectivity and to use as proof of the molecule's conformation. The square planar *cis*-Pt dichloride fragment of **1** and **2** is attached to two thiophenes and two [2,3-*b*]-TTs respectively, each through an ethoxycarbene carbon.

In **3b** and **4a**, the square planar *cis*-Pt dichloride fragment is attached to two [2,3-*b*]-TT spacers, in the case of the former

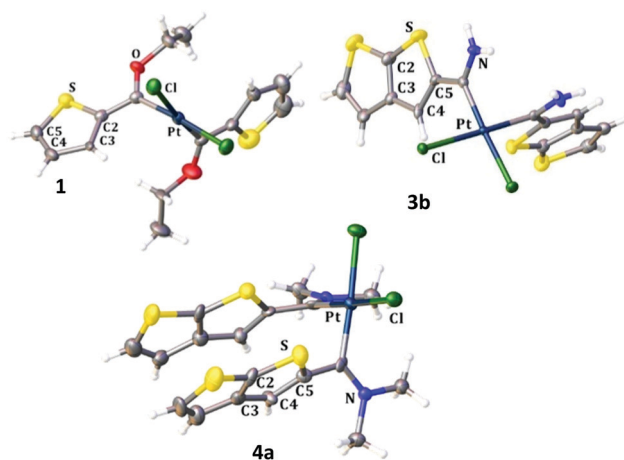


Fig. 3 The molecular structures of **1**, **3b** and **4a** with the atomic displacement ellipsoids shown at the 50% probability level.



Table 3 Selected bond lengths (Å) and angles (°) of **1**, **3b** and **4a**

Complex	1 ^a	3b ^a	4a ^a
Bond lengths			
M–C _{carb}	1.986(7), 1.945(9)	1.968(3), 1.964(2)	1.993(9), 1.98(1)
C _{carb} –O/N	1.285(9), 1.34(1)	1.303(4), 1.297(4)	1.30(1), 1.29(1)
Pt–Cl	2.372(3), 2.373(2)	2.3874(7), 2.3765(8)	2.363(3), 2.383(2)
C _{carb} –C2/C5	1.42(1), 1.39(1)	1.451(4), 1.449(4)	1.46(1), 1.49(1)
C2–C3	1.47(1), 1.43(1)	1.378(4), 1.383(4)	1.39(1), 1.37(2)
C3–C4	1.44(1), 1.40(1)	1.445(4), 1.414(4)	1.43(1), 1.42(1)
C4–C5	1.35(1), 1.36(2)	1.396(4), 1.375(4)	1.37(2), 1.36(2)
S–C2	1.728(7), 1.77(1)	1.703(3), 1.712(3)	1.71(1), 1.73(1)
S–C5	1.685(9), 1.69(1)	1.758(3), 1.747(3)	1.754(8), 1.731(9)
Bond angles			
M–C _{carb} –O/N	126.0(6), 127.5(6)	119.1(2), 121.3(2)	122.8(7), 125.5(7)
M–C _{carb} –C2/C5	121.1(6), 123.2(6)	122.8(2), 120.6(2)	117.2(7), 115.8(7)
O/N–C _{carb} –C2/C5	113.0(7), 109.3(7)	118.1(3), 118.2(3)	119.9(9), 118.6(8)
Torsion angles			
M–C _{carb} –C2/C5–C3/C4	14(1), 9(1)	5.4(4), –179.0(2)	–139(1), 116(1)
O/N–C _{carb} –C2/C5–C3/C4	–167.5(7), –170.7(8)	–174.6(3), 1.1(5)	46(2), –64(1)
Angle between two mean planes ^b	10.03, 9.76	4.18, 2.88	39.54, 61.34
Angle between two thienylene mean planes ^c	72.75	87.10	11.15

^a First set of data reported for first carbene fragment and the second for the second carbene fragment. ^b First mean plane drawn through C2, C3, C4 and C5, and the second through M, C_{carb} and O/N. ^c Mean plane drawn through C2, C3, C4 and C5 of each thienylene.

through aminocarbene carbons and the latter through dimethylaminocarbene carbons.

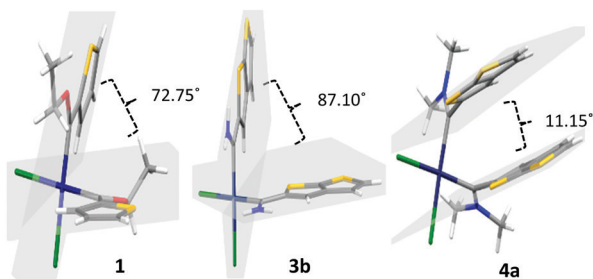
The ethoxycarbene complexes **1** and **2** have the *anti*-isomer arrangement in the solid state with their ethyl groups and metal moiety on the same side of the (M)C_{carb}–O(Et) bonds.^{23–26} In both structures the ethoxy substituents appear on the same side as the thienylene spacer's adjacent sulphur atom. In the case of the aminocarbene complex **3b**, the first amino group is on the same side as its thienylene spacer's adjacent sulphur atom and the second on the opposite side of its thienylene spacer's adjacent sulphur atom. For **P4w**, the dimethylamine group is on the same side as the sulphur atoms in the TT spacer (ESI,† Fig. S19), contradictory to what is observed for **4a** (Fig. 3 and 4) where the dimethylamine groups are remote from the sulphur atoms in the TT spacers. The thienylene spacer, carbene carbon, metal and amino fragment of **3b** (for both carbene fragments) are approximately in the same plane. The angle between a mean plane through C2, C3, C4 and C5 and a second through Pt, C_{carb} and N confirms this (Table 3). This is not the case in **1** and **4a**, and **P4w** and **5** (ESI†), where the angles between the two mean planes deviate from linearity as much as 10–89°. These results are also supported by the torsion angles reported in Table 3 and Table S6, ESI.† The two T and two TT fragments in

1 and **3b**, respectively, are approximately perpendicular to each other.

The angles between the fragments (mean plane drawn through C2, C3, C4 and C5 of each thienylene) are 72.75 and 87.10° individually (Fig. 4). The two carbene p_π-orbitals are also approximately perpendicular to each other and hence do not compete for the same π-interaction-orbital as the Pt center. This would explain why steric factors play such a small part in these carbene ligands. This is in contrast to the two TT fragments in **4a** where the spacers are almost parallel (11.15° angle between the fragments). The averaged Pt–C_{carb} bond lengths for Pt-carbene complexes in this study, **1**, **3b** and **4a**, are the same and independent of the type of thienylene spacer or ethoxy/amino/dimethylamine group present in the molecule (1.966(8), 1.966(3) and 1.987(9) Å respectively). Compared to a Pt^{II} bisethoxycarbene complex [PtCl₂{C(OEt)-*p*-C₆H₄NMe₂}₂] with an averaged Pt–C_{carb} bond length of 1.935 (16) Å, the former is slightly longer in length.⁸

In Pt cationic tris-dimethylaminocarbene complexes ([PtCl{C(NMe₂)-*p*-C₆H₄NMe₂}₃]⁺[W(CO)₅Cl][–] and [PtCl{C(NMe₂)-*p*-C₆H₄NMe₂}₃]⁺PF₆[–]) the carbene ligands *trans* to each other have longer averaged Pt–C_{carb} bond lengths, 2.053(4) and 2.055(4) Å respectively, compared to their singular carbene ligand *trans* to Cl, 1.975(6) and 1.973(4) Å respectively. The Pt–C_{carb} bond lengths in Pt cationic tris-dimethylaminocarbene complexes are longer compared to Pt biscarbene complexes (**1**, **3b**, **4a** and [PtCl₂{C(OEt)-*p*-C₆H₄NMe₂}₂]).⁸

The C_{carb}–C2/C5 bond lengths of **1** are shorter compared to **3b** and **4a** (Table 3), confirming that the ethoxycarbene complex is more dependent on electron density from the thienylene substituent to stabilize the carbene carbon compared to amino- and dimethylaminocarbene complexes. For **3b**, NH₂⋯S intramolecular interactions are observed (Fig. S20, ESI†) for the sulfur of the thienylene spacer that is *cis* to the NH₂ unit. This is not possible if the sulphurs of the thienylene spacer are *trans* to

Fig. 4 Angles between the thienylene fragments of **1**, **3b** and **4a**.

the NH₂ unit, instead intermolecular hydrogen bonding interactions occur between TT-H4 and NH with the oxygen of a co-crystallized THF molecule (2.510 and 2.091 Å, respectively). Thus, two different orientated TT spacers are observed.

Catalytic hydrosilylation

The well-studied and documented a hydrosilylation model reaction with phenylacetylene and triethylsilane is depicted in Scheme 2.^{9–11,14,27,28} Six possible products have been reported for the reaction; triethyl(1-phenylvinyl)silane (α -isomer), (*E*)-triethyl(styryl)silane (β -*E*-isomer), (*Z*)-triethyl(styryl)silane (β -*Z*-isomer), hydrogenated products (styrene and ethylbenzene) and a dehydrogenative silylation product (triethyl(phenylethynyl)silane). Pt^{II} NHC catalysts display almost exclusive selectivity for the β -*E* or α -isomers.^{11,14,27,29,30} Due to the lack of solubility and the ambiguity with regards to the purity/molecular structure of the aminocarbene complexes **3** and **4**, only the well-defined ethoxy-FCCs **1** and **2** were evaluated as catalyst precursors for phenylacetylene hydrosilylation with triethylsilane. The reactions in Tables 4 and 5 were performed in toluene-d₈, except for the neat experiments (entries 14 and 15, Table 4). A stability test was performed for **2** (entry 1, Table 4), in the absence of any substrate. After heating the reaction tube with **2** for 6 hours at 80 °C, no decomposition indicative of a Pt-catalyzed carbene self-dimerization product is observed.^{31,32}

Optimisation of the hydrosilylation reaction conditions were performed using **2** (entries 3–10, Table 4). The optimal reaction conditions were found to be 0.3 mol% catalyst loading at 80 °C for 2 hours (entry 9). Complete conversion was reached within this time, compared to some of the most active catalysts where 6 hours are required.⁹ Pronounced selectivity for the β -*E*-isomer was observed, as have been reported for most Pt^{II} catalysed hydrosilylation reactions.^{14,33} In the case of entry 9, product distribution (β -*E*/ α / β -*Z*) is determined as 74/23/3 (see NMR spectrum in Fig. S22, ESI†). By-products from the reaction; styrene, ethylbenzene and triethyl(phenylethynyl)silane, are reported in Table S8, ESI†.

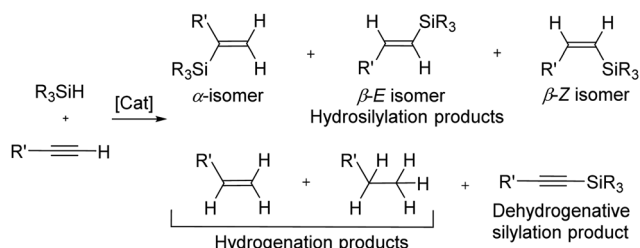
Styrene formed (up to 7% yield) during most of the optimization reactions, as long as the catalyst loading is high enough (>0.2 mol%) and the reaction time long enough (>1 h). Ethylbenzene was not observed and triethyl(phenylethynyl)silane is mostly observed in trace amounts (<1% yield). Changing the catalyst precursor to **1** (entry 11, Table 4) leads to a slight improvement in the % conversion and yield, but the selectivity is not influenced. The insignificantly different behaviour leads to the conclusion that there is virtually no difference between the

reactivity of the T- and TT-substituted carbene ligands. However, the presence of the Fischer carbene ligand is required for catalytic activity, as determined from comparison to the performance of the platinum precursors, K₂PtCl₄ (entry 12) and *cis*-[PtCl₂(NCMe)₂] (entry 13).

Observation of plausible intermediates of platinum complexes containing chelated acyclic aminocarbene ligands during hydrosilylation catalysis, has been reported previously.⁹ These intermediates represent either products of oxidative addition of the H–Si bond of the hydrosilane to the catalyst precursor's core or a product of the 1,2-alkyne insertion into the Pt–H bond of the catalyst core, already containing the silyl fragment (see Scheme S2, ESI†). K₂PtCl₄ and *cis*-[PtCl₂(NCMe)₂] did not perform as well as our platinum catalyst precursors, **2** and **1**, that display pronounced selectivity for one-to-two products. Performing the reactions neat (solvent free) with **2** (entry 14) and **1** (entry 15), led to reaction completion. No yield could be calculated for these reactions, but the product distribution could be determined as a ratio. Compared to entries 9 and 11, respectively, slightly more β -*E*-isomer and less β -*Z*-isomer formed. Complex **2** displayed high functional group tolerance as substrate screening was investigated (Table 5). Compared to hydrosilylation with phenylacetylene as substrate, entries 1–5 led to higher % yields of the hydrosilylation isomeric products.

Entry 7, carried out with *N*-Boc-propargylamine as substrate, yielded less hydrosilylation isomeric products. No products are obtained when using propargylamine and bis(trimethylsilyl)acetylene as substrates. Because of the high % yields obtained, the reaction time of selected substrates was decreased with the aim to decrease % yields to enable comparisons. The % yields of entries 9 and 12 (Table 5) were insignificantly influenced by the time change. In the case of internal alkyne, 3-hexyne (entry 10) and amine-functionalised alkyne, *N*-Boc-propargylamine (entry 11), a decrease in activity is seen, more extreme in the case of the latter. Selectivity of **2** for the β -*E*-isomer is better in entries 1, 2, 4 and 5 (Table 5), compared to hydrosilylation with phenylacetylene as substrate. The NMR spectrum of entry 5, Table 5 is displayed in Fig. S27, ESI†. Complete selectivity for the β -*E*-isomer is observed when the internal alkyne 3-hexyne is used as substrate, as the expected α -isomer formation is not possible. Selectivity for the β -*E*-isomer is poorer in the cases where 3-TMSO-1-propyne (entry 3) and *N*-Boc-propargylamine (entry 7) are used as substrates (TMSO = trimethylsulfoxide, Boc = *tert*-butoxycarbonyl). When the reaction time of selected substrates is decreased, a slightly higher selectivity for the β -*E*-isomer is observed. Assignments of ¹H NMR signals (Table S7, ESI†), for products obtained during hydrosilylation were made according to literature reports: phenylacetylene,^{14,34–37} 1-hexyne,^{38–41} 3-hexyne,^{42–45} 3-TMSO-1-propyne,⁴⁶ 5-hexyn-1-ol³⁸ and 5-chloro-1-pentyne.⁴⁷ The only evidence of a dehydrogenative silylation product is observed as a byproduct in the reaction using phenylacetylene as a substrate (triethyl(phenylethynyl)silane, 1.23 (9H, t, ²*J* 7.9)).³⁵

Comparison of the catalytic performance of **2** and **1** with recent examples of Pt^{II} NHC catalysts for this benchmark hydrosilylation reaction, reveals superior selectivity of the Pt^{II} FCCs **1** and **2** in the majority of cases.^{11,14,27,29,30} Similarly,



Scheme 2 Hydrosilylation of alkynes using hydrosilane.¹¹

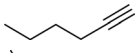
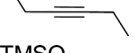
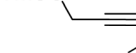
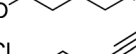
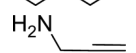
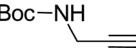
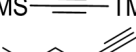
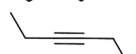
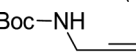
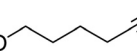




Table 4 Optimization of hydrosilylation using phenylacetylene and triethylsilane (variation of catalyst loading, temp., time, and catalyst precursor: **1**, **2**, *cis*-[PtCl₂(NCMe)₂], K₂PtCl₄)

Entry	Catalyst precursor	Catalyst loading (mol%)	Time (h)	Temp. (°C)	Conv. ^a (%)	Total% yield ^b /TON/TOF (h ⁻¹)	Product distribution β-E/α/β-Z (%)
1 ^{cd}	2	2	6	80	0	0/0/0	0/0/0
2 ^{ce}	—	—	6	80	25	1/0/0	100/0/0
3 ^e	2	1	6	80	98	83/83/14	74/24/2
4	2	0.5	6	80	97	91/182/30	75/23/2
5 ^e	2	0.3	6	80	99	87/290/48	75/23/2
6	2	0.2	6	80	40	39/195/33	41/56/3
7 ^e	2	0.3	6	40	16	5/17/3	60/40/0
8 ^e	2	0.3	3	80	98	85/283/94	74/24/2
9 ^e	2	0.3	2	80	94	81/270/135	74/23/3
10	2	0.3	1	80	48	41/137/137	71/27/2
11 ^e	1	0.3	2	80	98	83/277/138	73/23/4
12 ^e	K ₂ PtCl ₄	0.3	2	80	13	0/0/0	0/0/0
13	<i>cis</i> -[PtCl ₂ (NCMe) ₂]	0.3	2	80	52	44/147/73	50/45/5
14 ^f	2	0.3	2	80	—	—	76/22/2
15 ^f	1	0.3	2	80	—	—	77/22/1

^a Conversion as determined by NMR integration based on the two substrates (phenylacetylene and triethylsilane) and referenced to internal standard anisole. ^b Yield as determined from NMR integration based on the limiting substrate (most of the time phenylacetylene). ^c Experiments not performed in duplicate. ^d Substrate loading = 0. ^e An unidentified precipitate was observed. ^f Reactions were performed neat (no solvent). Complete conversion was observed, however no yield could be calculated.

Table 5 Substrate functional group tolerance and product distribution dependence on time (with **2** as catalyst precursor at 0.3 mol% catalyst loading in toluene-d₈ at 80 °C)

Entry	Substrate	Time (h)	Conv. (%)	Total % yield ^b /TON/TOF (h ⁻¹)	Product distribution β-E/α/β-Z (%)
1		2	99	94/313/157	76/21/3
2		2	100	100/333/167	99/0/1
3		2	99	94/313/157	61/37/2
4		2	99	98/327/163	88/11/1
5 ^a		2	100	87/290/145	81/16/3
6		2	6	0/0/0	0/0/0
7		2	73	73/243/122	69/31/0
8 ^a		2	13	0/0/0	0/0/0
9		1	98	95/317/317	86/12/2
10		1	86	86/287/287	99/0/1
11		1	38	36/120/120	72/28/0
12		1	99	96/320/320	89/10/1

^a An unidentified precipitate was observed.

the activity of the FCCs compares well with the state-of-the-art NHC complexes, as complete conversion is possible with 0.3 mol% catalyst loading at 80 °C for 2 hours, although some reports cite lower catalyst loading,^{11,14} or higher turnover numbers (TONs).⁹

Considering the evidence for vinylsilane product formation *via* the standard Chalk–Harrod mechanism, the same mechanism is proposed for **2** and **1** (Scheme S2, ESI†).^{9,34} Oxidative addition of

the silane to the Pt metal centre is followed by chloride ligand dissociation. Alkyne migratory 1,2-insertion occurs into the Pt–H bond, followed by reductive elimination to give the β-*E*-isomer. The α-isomer is formed through 2,1-insertion of the alkyne into the Pt–H bond, followed by reductive elimination. As the formation of the β-*Z*-isomer is negligible, the possibility of alkyne insertion into the Pt–Si bond, is discarded.

Finally, the recyclability of **2** was investigated. A catalytic experiment was done in duplicate with 0.3 mol% catalyst loading at 80 °C for 2 hours in toluene-d₈. After reaction completion/full conversion, substrates phenylacetylene and triethylsilane were added again, with the same equivalents as employed in the first batch reaction. This procedure was repeated four times, and the reaction still ran to completion and no decrease in activity was observed.

Conclusions

The number of carbene ligands that coordinate to the Pt^{II} metal, depends on the steric and electronic properties of the carbene ligand as determined by its substituents. In this study, mostly neutral mononuclear Pt^{II}-biscarbene complexes were obtained (**1**, **2**, **3a/b** and **4a/b**) from carbene transfer *via* group 6 FCC precursors. In the case of both the Pt-biscarbene complexes **3** and **4**, two geometric stereoisomers are observed. The formation of an insoluble cationic Pt triscarbene complex **4d** was only indicated for the transmetalation reaction from dimethylaminocarbene complexes.

This study reports the first utilization of Fischer carbene ligands coordinated to a Pt^{II} metal centre, as molecular catalyst precursors for alkyne hydrosilylation reactions. The Pt^{II} FCCs **1** and **2** were tested as catalyst precursors for the benchmark reaction of phenylacetylene with triethylsilane. Both (pre)catalysts exhibited good activity as complete conversion was reached in a short period of time, and a high functional group tolerance for the



alkyne substrates. At optimal reaction conditions, product distribution (β -E/ α / β -Z) was determined as 73/23/4 and 74/23/3, respectively. Notably, this selectivity is an improvement on that of known Pt^{II} NHC complexes, with comparable activity. The possibility of excluding solvent use in neat hydrosilylation reactions with **1**/**2** as catalyst precursors, proved possible with the additional advantage of improved selectivity for the β -E-isomer, while **2** can be reused for at least four batch hydrosilylation reactions, without any evidence of decomposition or decreased reactivity.

Experimental

General

All operations were carried out using standard Schlenk techniques or vacuum line techniques under an inert atmosphere of nitrogen or argon, using oven-dried glassware. Silica gel 60 (particle size 0.063–0.20 mm) was used as resin (stationary phase) for all column chromatography separations.

Chemical reagents and solvents

THF and diethyl ether were distilled over sodium wire and benzophenone under N₂ (g) atmosphere, hexane over sodium wire and DCM over CaH₂. Other chemicals were used as they were commercially supplied by Sigma Aldrich and Strem Chemicals. The *n*-BuLi used in syntheses was from a stock 1.6 M solution in hexane.

Triethyloxonium tetrafluoroborate was prepared according to literature procedure and stored in diethyl ether under Ar (g).⁴⁸ Boron trifluoride etherate was distilled before use. Pt(COD)Cl₂,⁴⁹ *cis*-[PtCl₂(NCMe)₂],⁵⁰ and group 6 FCC precursors^{21,51–53} [Cr(CO)₅{C(OEt)-2-C₄H₉S₂}] **P1_{Cr}**, [Cr(CO)₅{C(OEt)-5-C₆H₃S₂}] **P2_{Cr}**, [W(CO)₅{C(OEt)-5-C₆H₃S₂}] **P2_W**, and [W(CO)₅{C(NH₂)-5-C₆H₃S₂}] **P3_W** were prepared according to literature procedures. The synthesis and characterization of [Cr(CO)₅{C(NMe₂)-5-C₆H₃S₂}] **P4_{Cr}** and [W(CO)₅{C(NMe₂)-5-C₆H₃S₂}] **P4_W** are reported in the ESI.[†]

Synthesis and characterization of Fischer carbene complexes

Synthesis of platinum(II) ethoxycarbene complexes of thiophene

Excess **P1_{Cr}** (3.00 g, 9.0 mmol) and Pt(COD)Cl₂ (1.53 g, 4.1 mmol) were dissolved in 20 mL dried DCM (degassed for 15 min) and allowed to reflux under an inert atmosphere at 50 °C for 24–30 hours. The solvent was removed under vacuum and the reaction mixture dissolved in a minimal amount of DCM. The product was cannula filtered and triturated with hexane. The product was repeatedly washed with large amounts of dry ether to separate unreacted Pt(COD)Cl₂ from **1** (listed in ESI,[†] Table S2), before being dried under vacuum.

1: $\delta^1\text{H}$ (400.13 MHz; CDCl₃; Me₄Si) 8.09 (2 H, d, $^3J_{5,4}$ 4.7, H5), 7.28 (2 H, dd, $^3J_{4,7}$ 4.7, 3.7, H4), 8.69 (2 H, d, $^3J_{3,4}$ 3.7, H3), 5.60 (4 H, s, br, CH₂), 1.59 (6 H, t, J 6.8, CH₃). $\delta^1\text{H}$ (300.13 MHz; CD₂Cl₂; Me₄Si) 8.13 (2 H, dd, $^3J_{5,4}$ 5.0, $^4J_{5,3}$ 0.9, H5), 7.31 (2 H, dd, $^3J_{4,7}$ 5.0, 3.8, H4), 8.68 (2 H, d, $^3J_{3,4}$ 3.8, H3), 5.54 (4 H, s, br,

CH₂), 1.59 (6 H, t, J 7.1, CH₃). $\delta^{13}\text{C}$ (75.468 MHz; CD₂Cl₂; Me₄Si) 235.2 (C_{carb}), 142.5 (C5), 130.4 (C4), 145.4 (C3), 150.5 (C2), 80.5 (CH₂), 14.8 and 14.8 (CH₃). m/z (C₁₄H₁₆O₂Cl₂S₂Pt, 546.39 g mol⁻¹) calculated: 736.9030, found: 737.1392 (30%, [M₂{C(OEt)C₄H₃S₂}]⁻).

Synthesis of platinum(II) ethoxycarbene complexes of [2,3-*b*]-TT

The same reaction method as above was applied to excess **P2_{Cr}** (0.17 g, 0.4 mmol) and Pt(COD)Cl₂ (0.06 g, 0.2 mmol). Instead of using large amounts of ether, the product was repeatedly washed with minimum amounts of chloroform, followed by a single ether wash. Dissolved in DCM, the product (listed in ESI,[†] Table S3) was dried on MgSO₄, filtered and dried under vacuum.

2: λ_{max} (CH₂Cl₂)/nm 400 (ϵ /dm³ mol⁻¹ cm⁻¹ 33140), 355 (43120). $\delta^1\text{H}$ (400.13 MHz; CDCl₃; Me₄Si) 9.08 (2H, s, H4), 7.44 (2H, d, $^3J_{5',4'}$ 5.2, H5'), 7.35 (2H, s, br, H4'), 5.77 and 5.18 (2H + 2H, s, br, CH₂), 1.59 (6H, s, br, CH₃). $\delta^1\text{H}$ (500.139 MHz; CD₂Cl₂; Me₄Si) 9.03 (2H, s, H4), 7.49 (2H, d, $^3J_{5',4'}$ 5.1, H5'), 7.39 (2H, s, br, H4'), 5.73 and 5.21 (2H + 2H, s, br, CH₂), 1.58 (6H, s, br, CH₃). $\delta^1\text{H}$ (400.13 MHz; CD₂Cl₂; Me₄Si at 2 °C) 9.05 (2H, s, H4), 7.49 (2H, s, br, H5'), 7.39 (2H, s, br, H4'), 5.73 and 5.14 (2H + 2H, s, br, CH₂), 1.61 (6H, s, br, CH₃). $\delta^{13}\text{C}$ (125.75 MHz; CD₂Cl₂; Me₄Si) 233.2 (br, C_{carb}), 153.6 (C5), 140.2 (br, C4), 152.3 and 148.3 (C3 and C2), 131.9 (C5'), 122.1 (C4'), 80.1 (CH₂), 14.9 (CH₃). m/z (C₁₈H₁₆O₂S₄Cl₂Pt, 658.56 g mol⁻¹) calculated: 691.8747, found: 691.8950 (35%, [M + Cl]⁻).

Synthesis of platinum(II) aminocarbene complexes of [2,3-*b*]-TT

The same reaction method as above was applied to excess **P3_W** (0.11 g, 0.22 mmol) and Pt(COD)Cl₂ (0.03 g, 0.1 mmol). A cream brown reaction mixture was obtained when minimum amounts of DCM were added. The product was washed repeatedly with DCM and ether using cannula filtration. The product was dried under vacuum, dissolved in THF and filtered through Celite and MgSO₄ before being put up for crystals. The products isolated are listed in ESI,[†] Table S4.

3a: ν_{NH} (KBr pellet)/cm⁻¹ 3294s, br (ν_{as}) and 3210s, br (ν_{s}). $\delta^1\text{H}$ (500.139 MHz; (CD₃)₂SO; Me₄Si) 10.77 and 10.61 (2H + 2H, s, br, NH₂), 8.26 (2H, s, H4), 7.66 (2H, d, $^3J_{5',4'}$ 5.3, H5'), 7.40 (2H, d, $^3J_{4',5'}$ 5.3, H4'). $\delta^{13}\text{C}$ (125.75 MHz; (CD₃)₂SO; Me₄Si) 196.5 (C_{carb}), 150.8 (C5), 124.2 (C4), 146.0 and 145.8 (C3 and C2), 130.9 (C5'), 121.0 (C4'). m/z (C₁₄H₁₀N₂Cl₂S₄Pt, 600.49 g mol⁻¹) calculated: 677.7935, found: 677.7938 (9%, [M + Br]⁻).

3b: $\delta^1\text{H}$ (500.139 MHz; (CD₃)₂SO; Me₄Si) 11.42 and 11.18 (2H + 2H, s, br, NH₂), 8.56 and 8.46 (2H, s, H4), 7.73 and 7.72 (2H, d, $^3J_{5',4'}$ 5.3, H5'), 7.46 and 7.43 (2H, d, $^3J_{4',5'}$ 5.3, H4').

Synthesis of platinum(II) dimethylamine-carbene complexes of [2,3-*b*]-TT

The same reaction method was applied to excess **P4_{Cr}** (0.17 g, 0.45 mmol) and Pt(COD)Cl₂ (0.056 g, 0.15 mmol). The solvent was removed under vacuum and the reaction mixture washed with minimal amounts of DCM, chloroform and ether. The product (listed in ESI,[†] Table S5) was dried under vacuum. Filtering the product through silica gel, with acetone as eluent, causes the product to decompose to the corresponding organic ester product **5**.



4a: $\delta^1\text{H}$ (300.13 MHz; CDCl_3 ; Me_4Si) 8.06 (2H, s, H4), 7.45 (2H, d, 3J 5.3, H5'), 7.35 (2H, d, 3J 5.3, H4'), 4.22 and 3.86 (6H + 6H, s, NCH_3). $\delta^1\text{H}$ (300.13 MHz; $(\text{CD}_3)_2\text{SO}$; Me_4Si) 8.00 (2 H, s, H4), 7.73 (2 H, d, 3J 5.3, H5'), 7.45 (2H, d, 3J 5.3, H4'), 4.06 and 3.77 (6H + 6H, s, NMe_2). m/z ($\text{C}_{18}\text{H}_{18}\text{N}_2\text{Cl}_2\text{S}_4\text{Pt}$, 656.59 g mol^{-1}) calculated: 688.7982, found: 688.9038 (12%, $[\text{M} + \text{Br-NMe}_2\text{H}]^-$), calculated: 661.9028, found: 661.9876 (10%, $[\text{M} + \text{Br-2Cl-2H}]^-$).

4b: $\delta^1\text{H}$ (400.13 MHz; CDCl_3 ; Me_4Si) 7.61 (2H, s, H4), 7.38 (2H, d, 3J 5.3, H5'), 7.29 (2 H, d, 3J 5.3, H4'), 3.30 (12H, s, NMe_2). $\delta^1\text{H}$ (500.139 MHz; $(\text{CD}_3)_2\text{SO}$; Me_4Si) 7.80 (2H, s, H4), 7.70 (2H, d, 3J 5.2, H5'), 7.41 (2H, d, 3J 5.2, H4'), 4.15 and 3.65 (6H + 6H, s, NMe_2).

4d: $\delta^1\text{H}$ (300.13 MHz; $(\text{CD}_3)_2\text{SO}$; Me_4Si) 7.65 (2H, s, br, H4 (*trans to carbene ligand*)), 7.37 (3H, s, br, H5' (*trans to carbene ligand*) + H4 (*trans to Cl*)), 7.26 (2H, s, br, H4' (*trans to carbene ligand*)), 6.87 (1H, s, br, H5' (*trans to Cl*)), 6.78 (1H, s, br, H4' (*trans to Cl*)), 4.10 and 3.63 (6H + 6H, s, br, NMe_2 (*trans to carbene ligand*)), 3.38 and 3.30 (3H and 3H, s, br, NCH_3 (*trans to Cl*)).

5: ν_{CO} (hexane)/ cm^{-1} 1639m, br (C=O stretching vibration). $\delta^1\text{H}$ (300.13 MHz; CDCl_3 ; Me_4Si) 7.48 (1H, s, H4), 7.36 (1H, d, $^3J_{5',4'}$ 5.3, H5'), 7.21 (1H, d, $^3J_{4',5'}$ 5.3, H4'), 3.21 (6H, s, br, NMe_2). $\delta^{13}\text{C}$ (75.468 MHz; CDCl_3 ; Me_4Si) 164.1 ($(\text{NMe}_2)\text{C}(\text{O})$), 145.9 (C5), 121.8 and 121.8 (C4), 141.1 and 140.2 (C3 and C2), 128.6 (C5'), 120.3 (C4'), 38.0 (br, NMe_2). m/z ($\text{C}_9\text{H}_9\text{NOS}_2$, 211.3 g mol^{-1}) calculated: 212.0204, found: 212.0264 (84%, $[\text{M} + \text{H}]^+$), calculated: 234.0023, found: 234.0091 (100%, $[\text{M} + \text{Na}]^+$).

Catalytic hydrosilylation reactions

A dry high pressure NMR tube fitted with a J. Young valve, was charged with the (pre)catalyst precursor, alkyne, triethylsilane and internal standard in toluene- d_8 under an atmosphere of argon, before heating. Each reaction contained triethylsilane (40.0 μL , 0.25 mmol) and 0.2 mL toluene- d_8 . Anisole was used as internal standard (27 μL , 0.25 mmol) and was integrated in the proton NMR spectra to represent three protons (area: 3.34–3.31 or 3.36–3.30 ppm). No triethylsilane was added in entry 1 (Table 4) and entries 14 and 15 (Table 4) were done solvent free. After a predetermined time at a certain temperature (80 $^\circ\text{C}$, except entry. 7, Table 4, was performed at 40 $^\circ\text{C}$), the NMR data are collected and analysed. Reaction conditions applied to individual reactions are reported in Table S8, ESI.[†] After the reactions were completed the solutions appeared pale yellow, indicating the presence of hydrosilylation isomeric products that formed.

A descriptive example for a performed catalytic run (entry 9, Table 4) is as follows: 0.3 mol% of **2**, phenylacetylene (27.5 μL , 0.25 mmol), triethylsilane (40.0 μL , 0.25 mmol), anisole (27.0 μL , 0.25 mmol) and 0.2 mL toluene- d_8 was added to a high pressure NMR tube, under an atmosphere of argon. The sealed NMR tube was then placed in an oil bath set at 80 $^\circ\text{C}$ for 2 hours. The NMR tube is allowed to reach RT before NMR spectra were collected. Catalytic reactions were performed in duplicate, unless stated otherwise, and the averaged results reported.

Characterization and analytical techniques

Ultraviolet spectra could not be obtained for **1**, **3**, **4** and **5** (these compounds are yellow to colourless when diluted to 0.01 mM in 10 mL of DCM and **3** and **4** are insoluble in DCM). **4d** did not ionize during mass spectrometric (MS) analysis. Dimerization of **1** through bridging chlorido ligands was observed in the MS of the sample.

Nuclear magnetic resonance spectroscopy. NMR spectra were recorded on Bruker AVANCE 500, Ultrashield Plus 400 AVANCE 3 and Ultrashield 300 AVANCE 3 spectrometers, at 25 $^\circ\text{C}$. The ^1H NMR spectra were recorded at 500.139, 400.13 or 300.13 MHz, and the ^{13}C NMR spectra at 125.75, 100.613 or 75.468 MHz, respectively. CDCl_3 , CD_2Cl_2 and $(\text{CD}_3)_2\text{SO}$ were used as solvent. For the samples measured in CDCl_3 , chemical shifts (reported as δ (ppm) downfield from Me_4Si) are referenced at 7.26 ppm for δH and 77.0 ppm for δC . The CD_2Cl_2 reference signals are at 5.32 ppm for δH and 54.0 ppm for δC , and the $(\text{CD}_3)_2\text{SO}$ reference signals are at 2.50 ppm for δH and 39.5 ppm for δC . An additional low temperature ^1H NMR spectrum of **2** was measured in CD_2Cl_2 at 2 $^\circ\text{C}$. The toluene- d_8 reference signal is at 2.09 ppm for δH (hydrosilylation reactions). Coupling constants (J) are reported in Hz. Preparation of the samples was carried out under Ar(g) and the NMR tubes were sealed before data collection. The ^1H NMR data are reported in the format: chemical shift (integration, multiplicity, coupling constant, assignment) and the ^{13}C NMR data in the format: chemical shift (assignment), in the order of assignments. The spectral coupling patterns are: s – singlet, d – doublet, t – triplet and br – broad.

First-order analysis was carried out to assign signals of the ^1H NMR spectra. Additional 2D [^1H , ^1H] COSY NMR experiments were done where confirmation of the proton assignments were required. Assigning the carbon chemical shifts, obtained from proton-decoupled ^{13}C NMR spectra, was possible with the assistance of 2D [^1H , ^{13}C] HSQC and 2D [^1H , ^{13}C] HMBC NMR experiments (see ESI,[†] Section S3). Standard Bruker pulse programs were used in the experiments.

Fourier-transform infrared spectroscopy. Infrared spectroscopy was performed on a Bruker ALPHA FT-IR spectrophotometer with a NaCl cell, using dried hexane as solvent. Insoluble samples were measured in the solid state (KBr pellets). KBr pellets are pressed from dry homogeneously powdered KBr containing sample in 0.2–1% concentration. The absorptions were measured from 400–4000 cm^{-1} . The IR data are reported in the format: absorption intensity (assignment) in the order of highest to lowest wavenumber. The wave intensities are: w – weak, m – medium, s – strong, sh – shoulder and br – broad.

High-resolution mass spectrometry. Mass spectral analyses were performed on a Waters[®] Synapt G2 high definition mass spectrometer (HDMS) that consists of a Waters Acquity Ultra Performance Liquid Chromatography (UPLC[®]) system hyphenated to a quadrupole-time-of-flight (QTOF) instrument. Data acquisition and processing was carried out with MassLynxTM (version 4.1) software. A leucine enkephalin solution (2 pg μL^{-1} , m/z 555.2693) was used as an internal lock mass control standard.



to compensate for instrumental drift and ensure good mass accuracy. The internal control was directly infused into the source through a secondary orthogonal electrospray ionization (ESI) probe to allowing intermittent sampling. Flow injection analysis (FIA, 0.4 mL min⁻¹ flow rate) with the injection volume set at 5 µL. Samples were made up in ultra-purity liquid chromatography methanol to an approximate concentration of 10 µg mL⁻¹. The methanol was spiked with 0.1% formic acid and used throughout the 1 min run. The capillary voltage for the ESI source was set at 2.8 kV and 2.6 kV for positive and negative mode ionization, respectively. The source temperature was set at 110 °C, the sampling cone voltage at 25 V, extraction cone voltage at 4.0 V and cone gas (nitrogen) flow at 10.0 L h⁻¹. The desolvation temperature was set at 300 °C with a gas (nitrogen) flow of 600.0 L h⁻¹. The mass to charge ratios (*m/z*) were measured in the range of 50–1500 Da with the raw data presented in the form of a centroid profile (scans collected every 0.3 seconds). A negative electron spray was employed as the ionization technique, but positive electron spray was required for 5. The MS data are reported in the format: calculated mass, found mass (percentage intensity, fragmentation) in the order of highest to lowest mass to charge ratio.

UV-Vis spectroscopy

Measurements were performed on 10 mL DCM solutions of 0.01 mM analyte concentration at 25 °C. Absorptions were measured in the range 200–1000 nm using a UV-Vis spectrophotometer Specord 200 plus. WinASPECT PLUS (version 4.2) software was used for data visualization.

X-ray diffraction analysis

Single crystal diffraction data for **P4_w**, **2**, **3b** and **5**, were collected at 150 K on a Bruker D8 Venture diffractometer with a kappa geometry goniometer and a Photon 100 CMOS detector using a Mo-K α I μ S.micro focus source. Data were reduced and scaled using SAINT and absorption intensity corrections were performed using SADABS (APEX III control software).⁵⁴ Single crystals of **1** and **4a** were analyzed on a Rigaku XtaLAB Synergy R diffractometer, with a rotating-anode X-ray source and a HyPix CCD detector. Data reduction and absorption were carried out using the CrysAlisPro (version 1.171.40.23a) software package.⁵⁵ X-ray diffraction measurements were all performed at 150 K (except for **4a** at 293 K) using an Oxford Cryogenics Cryostat. All structures were solved by an intrinsic phasing algorithm using SHELXTS⁵⁶ and were refined by full-matrix least-squares methods based on *F*² using SHELXL.⁵⁷ All non-hydrogen atoms were refined anisotropically. All hydrogen atoms were placed in idealized positions and refined using riding models. The X-ray crystallographic coordinates for the structures of compounds **P4_w**, **1**, **2**, **3b**, **4a** and **5** have been deposited at the Cambridge Crystallographic Data Centre (CCDC), with deposition numbers CSD 2061163–2061168.

Conflicts of interest

There are no conflicts to declare.

Acknowledgements

The authors gratefully acknowledge the National Research Foundation, South Africa (NRF 105740; NRF 105529, NRF 87788 and NRF 9772) and Sasol Technology R&D Pty. Ltd. (South Africa) for financial support.

References

- 1 L. Chugaev and M. Skanavy-Grigorizeva, *Russ. Chem. Soc.*, 1915, **47**, 776.
- 2 L. Chugaev, M. Skanavy-Grigorizeva and A. Posniak, *Z. Anorg. Allg. Chem.*, 1925, **148**, 37.
- 3 W. M. Butler, J. H. Enemark, J. Parks and A. L. Balch, *Inorg. Chem.*, 1973, **12**, 451.
- 4 E. M. Badley, J. Chatt, R. L. Richards and G. A. Sim, *J. Chem. Soc. D*, 1969, **53**, 1322.
- 5 M. H. Chisholm and H. C. Clark, *Inorg. Chem.*, 1971, **10**, 1711.
- 6 M. Werner, T. Lis, C. Bruhn, R. Lindner and D. Steinborn, *Organometallics*, 2006, **25**, 5946.
- 7 M. P. López-Alberca, M. J. Mancheño, I. Fernández, M. Gómez-Gallego, M. A. Sierra and R. Torres, *Chem. – Eur. J.*, 2009, **15**, 3595.
- 8 N. Weststrate, *Structural and electronic features of tungsten(0) and platinum(II) complexes with Fischer carbene ligands*, PhD thesis, University of Pretoria, Pretoria, 2017.
- 9 R. S. Chay, B. G. M. Rocha, A. J. L. Pombeiro, V. Y. Kukushkin and K. V. Luzyanin, *ACS Omega*, 2018, **3**, 863.
- 10 K. Stefanowska, A. Franczyk, J. Szyling, K. Salamon, B. Marciniak and J. Walkowiak, *J. Catal.*, 2017, **356**, 206.
- 11 J. J. Hu, F. Li and T. S. A. Hor, *Organometallics*, 2009, **28**, 1212.
- 12 G. De Bo, G. Berthon-Gelloz, B. Tinant and I. E. Markó, *Organometallics*, 2006, **25**, 1881.
- 13 C. Xu, B. Huang, T. Yan and M. Cai, *Green Chem.*, 2018, **20**, 391.
- 14 B. G. M. Rocha, E. A. Valishina, R. S. Chay, M. F. C. Guedes Da Silva, T. M. Buslaeva, A. J. L. Pombeiro, V. Y. Kukushkin and K. V. Luzyanin, *J. Catal.*, 2014, **309**, 79.
- 15 F. Alonso, R. Buitrago, Y. Moglie, J. Ruiz-Martínez, A. Sepúlveda-Escribano and M. Yus, *J. Organomet. Chem.*, 2011, **696**, 368.
- 16 M. Chauhan, B. J. Hauck, L. P. Keller and P. Boudjouk, *J. Organomet. Chem.*, 2002, **645**, 1.
- 17 N. Nakata, M. Sakashita, C. Komatsubara and A. Ishii, *Eur. J. Inorg. Chem.*, 2010, 447.
- 18 E. Bolbat, K. Suarez-Alcantara, S. E. Canton and O. F. Wendt, *Inorg. Chim. Acta*, 2016, **445**, 129.
- 19 A. M. Voutchkova, M. Feliz, E. Clot, O. Eisenstein and R. H. Crabtree, *J. Am. Chem. Soc.*, 2007, **129**, 12834.
- 20 F. Hanasaka, Y. Tanabe, K. I. Fujita and R. Yamaguchi, *Organometallics*, 2006, **25**, 826.
- 21 Z. Lamprecht, *Fischer carbene complexes of 3,3'-bithiophene and thieno[2,3-*b*]thiophene*, MSc dissertation, University of Pretoria, Pretoria, 2015.



- 22 Z. Lamprecht, F. P. Malan, D. C. Liles, S. Lotz and D. I. Bezuidenhout, *J. Organomet. Chem.*, 2020, **925**, 121466.
- 23 D. M. Andrada, M. E. Zoloff Michoff, I. Fernández, A. M. Granados and M. A. Sierra, *Organometallics*, 2007, **26**, 5854.
- 24 I. Fernández, F. P. Cossio, A. Arrieta, B. Lecea, M. J. Mancheño and M. A. Sierra, *Organometallics*, 2006, **23**, 1065.
- 25 N. Lugan, I. Fernández, R. Brousses, D. A. Valyaev, G. Lavigne and N. A. Ustynyuk, *Dalton Trans.*, 2013, **42**, 898.
- 26 D. A. Valyaev, R. Brousses, N. Lugan, I. Fernández and M. A. Sierra, *Chem. – Eur. J.*, 2011, **17**, 6602.
- 27 M. Poyatos, A. Maisse-François, S. Bellemin-Lapponnaz and L. H. Gade, *Organometallics*, 2006, **25**, 2634.
- 28 L. Yong, K. Kirleis and H. Butenschön, *Adv. Synth. Catal.*, 2006, **348**, 833.
- 29 F. Zhang, Y. Bai, X. Yang, J. Li and J. Peng, *Phosphorus, Sulfur Silicon Relat. Elem.*, 2017, **192**, 1271.
- 30 C. Lu, S. Gu, W. Chen and H. Qiu, *Dalton Trans.*, 2010, **39**, 4198.
- 31 M. P. López-Alberca, M. J. Mancheño, I. Fernández, M. Gómez-Gallego, M. A. Sierra and R. Torres, *Org. Lett.*, 2007, **9**, 1757.
- 32 M. A. Sierra, J. C. del Amo, M. J. Mancheño and M. Gómez-Gallego, *J. Am. Chem. Soc.*, 2001, **123**, 851.
- 33 G. Berthon-Gelloz, J. M. Schumers, G. De Bo and I. E. Markó, *J. Org. Chem.*, 2008, **73**, 4190.
- 34 A. Tyagi, S. Yadav, P. Daw, C. Ravi and J. K. Bera, *Polyhedron*, 2019, **172**, 167.
- 35 M. Wissing and A. Studer, *Chem. – Eur. J.*, 2019, **25**, 5870.
- 36 H. Liang, Y.-X. Ji, R.-H. Wang, Z.-H. Zhang and B. Zhang, *Org. Lett.*, 2019, **21**, 2750.
- 37 K. H. Lee, B. Lee, K. R. Lee, M. H. Yi and N. H. Hur, *Chem. Commun.*, 2012, **48**, 4414.
- 38 X. Zhao, D. Yang, Y. Zhang, B. Wang and J. Qu, *Org. Lett.*, 2018, **20**, 5357.
- 39 S. V. Maifeld, M. N. Tran and D. Lee, *Tetrahedron Lett.*, 2005, **46**, 105.
- 40 S. Schwieger, R. Herzog, C. Wagner and D. Steinborn, *J. Organomet. Chem.*, 2009, **694**, 3548.
- 41 Z. Zhang, T. Xiao, H. Al-Megren, S. A. Aldrees, M. Al-Kinany, V. L. Kuznetsov, M. L. Kuznetsov and P. P. Edwards, *Chem. Commun.*, 2017, **53**, 4026.
- 42 R. Cano, M. Yus and D. J. Ramón, *ACS Catal.*, 2012, **2**, 1070.
- 43 K. Jakobsson, T. Chu and G. I. Nikonov, *ACS Catal.*, 2016, **6**, 7350.
- 44 K. M. McWilliams and R. J. Angelici, *Organometallics*, 2007, **26**, 5111.
- 45 R. J. Abraham, M. Canton and L. Griffiths, *Magn. Reson. Chem.*, 2001, **39**, 421.
- 46 Z. Gan, Y. Wu, L. Gao, X. Sun, J. Lei, Z. Song and L. Li, *Tetrahedron*, 2012, **68**, 6928.
- 47 R. Takeuchi, S. Nitta and D. Watanabe, *J. Org. Chem.*, 1995, **60**, 3045.
- 48 H. Meerwein, *Org. Synth.*, 1966, **46**, 113.
- 49 H. C. Clark and L. E. Manzer, *J. Organomet. Chem.*, 1973, **59**, 411.
- 50 F. P. Fanizzi, F. P. Intini, L. Maresca and G. Natile, *J. Chem. Soc., Dalton Trans.*, 1990, 199.
- 51 J. A. Connor and E. M. Jones, *J. Chem. Soc. A*, 1971, 1974.
- 52 Z. Lamprecht, N. A. van Jaarsveld, D. I. Bezuidenhout, D. C. Liles and S. Lotz, *Dalton Trans.*, 2015, **44**, 19218.
- 53 L. Yang, P. Ye, W. Li, W. Zhang, Q. Guan, C. Ye, T. Dong, X. Wu, W. Zhao, X. Gu, Q. Peng, B. Tang and H. Huang, *Adv. Opt. Mater.*, 2018, **6**, 1.
- 54 APEX3. (including SAINT and SADABS). BrukerAXS Inc., Madison, WI 2016.
- 55 Rigaku Oxford Diffraction. Rigaku Corporation: Oxford, UK 2018.
- 56 G. M. Sheldrick, *Acta Crystallogr., Sect. A: Found. Adv.*, 2015, **71**, 3.
- 57 G. M. Sheldrick, *Acta Crystallogr., Sect. C: Struct. Chem.*, 2015, **71**, 3.

